Millimeter and Submillimeter Wave Spectroscopy*

CHARLES A. BURRUS† AND WALTER GORDY
Department of Physics, Duke University, Durham, North Carolina
(Received September 19, 1955)

Rotational lines of several linear molecules have been measured with high precision in the region of 0.8- to 2.0-mm wavelength. The energy source for this region is a silicon crystal multiplier driven by a centimeter-wave klystron. A silicon crystal was also used as the detector. An evacuated bolometer detector was developed for the 3-mm wave region and was used to detect rotational lines down to 2.0 mm. Although its sensitivity is lower than that of the crystal detector, the bolometer will be useful for absolute power measurements in the shorter millimeter region.

INTRODUCTION

EARLY in 1954 we reported[1] extension of the microwave (radio) region down to a wavelength of 0.77 mm (389 000 Mc/sec). Between 0.77 mm and 1.0 mm several transitions of OCS were measured to seven significant figures with a frequency standard monitored by the 5-Mc/sec frequency of station WWV. During the same year Genzel and Eckhardt,[2] at Frankfort, Germany, extended infrared (optical) measurements of spectral frequencies up to wavelengths of 0.99 mm, where a rotational transition of H_2S was measured to 2 figures with a heat source and grating. Thus in 1954, optical and radio measurements of spectral lines actually met and overlapped for the first time, although as early as 1923 energy from an impractical spark gap oscillator was detected in this last spectral gap by Nichols and Tear.[3]

No further extension of the upper frequency bounds of the radio measurements is made in the present work. Instead, extensions of the submillimeter wave measurements to several other substances are made. The present measurements provide secondary frequency standards for optical spectroscopists at many points in the overlapping 0.77–1.0 mm region. They also allow accurate evaluation of the centrifugal stretching constants of a number of simple linear molecules, and thus indirectly they provide secondary standard markers all over the infrared region.

Measurements of l-type doubling to very high J values are made on some of the molecules in excited bending-vibrational modes. These measurements provide a test of the theory of interaction between rotation and vibration.

A bolometer has been constructed for the shorter millimeter wave region and extensive comparisons with crystal detection made. Effects of crystal biasing on the detector and multiplier crystals have been studied.

EXPERIMENTAL METHODS

The crystal multiplier and detector components are essentially those described by King and Gordy.[4] The principal change from the previous description is that the detector for the measurements below 1.5 mm is constructed from a smaller wave guide (inside dimensions 0.045×0.022 in.) to cut out the noise and confusion of the lower harmonics. The crystal size was also further reduced approximately in proportion to the reduction in wave-guide dimensions. The waveguide cell used in the present work was only 10 cm in length, and was made of G-band guide (inside dimensions 0.075×0.034 in.). The cell volume was therefore only 0.17 cc.

It was found that crystal biasing could be used to facilitate tuning of the multiplier assembly. Approximately 3 to 5 volts dc was applied to the "cat whisker" probe with the positive pole to the whisker. The OCS or other lines employed for tuning the assembly were used to find the optimum bias voltage. Care must be exercised to prevent burning the whisker point by

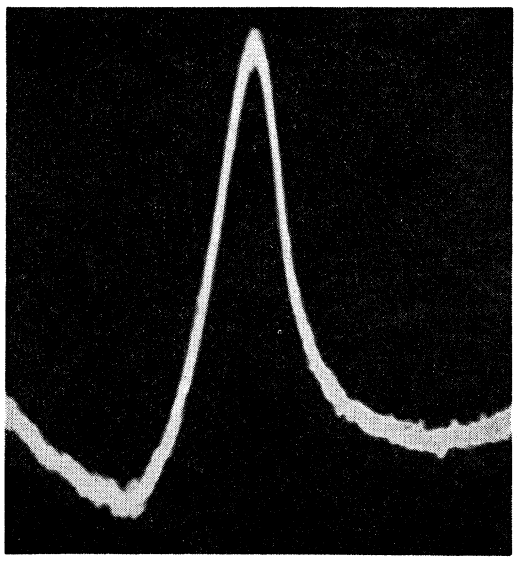

FIG. 1. Cathode-ray tracing of the $J=7\rightarrow8$ transition of OCS at 3.08-mm wavelength as obtained with a bolometer detector.

* This research was supported by The United States Air Force through the Office of Scientific Research of the Air Research and Development Command.

† Present address: Bell Telephone Laboratory, Holmdel Radio Laboratory, Red Bank, New Jersey.

[1] C. A. Burrus and W. Gordy, Phys. Rev. **93**, 897 (1954).

[2] L. Genzel and W. Eckhardt, Z. Physik **139**, 592 (1954).

[3] E. F. Nichols and J. D. Tear, Phys. Rev. **21**, 587 (1923).

[4] W. C. King and W. Gordy, Phys. Rev. **90**, 319 (1953); **93**, 407 (1954).

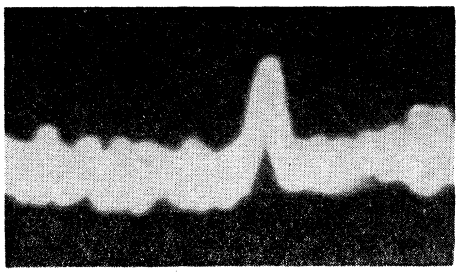

FIG. 2. Cathode-ray tracing of the $J=23\rightarrow24$ transition of $Cl^{35}CN$ at 1.05-mm wavelength obtained with a crystal detector and the 12th harmonic power of a 2K33 klystron.

overbiasing. A gain in signal-to-noise of absorption lines as much as 2 was sometimes obtained with crystal biasing. Nevertheless, it is not certain that any gain would be realized by biasing a perfectly tuned system.

A bolometer detector was constructed for the 3-mm wave region. Its sensitivity was found to be below that obtainable with the crystal detector. Nevertheless, its sensitivity is adequate for power measurements. Figure 1 shows an oscilloscope trace of the 3-mm wave line of OCS obtained with the bolometer detector. Other OCS lines down to 2 mm were detected with the same bolometer using a phase-lock-in amplifier and an automatic recorder. An increase of about 2 in the signal-to-noise ratio was obtained by evacuation of the bolometer.

TABLE I. HCN and DCN.

Molecule	Tube harmonic	Transition $J\rightarrow J+1$	Measured frequency ν_0(Mc/sec)[a]	Calculated frequency ν_0(Mc/sec)[b]	Wavelength (mm)
HCN	4	0→1	88 631.62±0.20	88 631.62	3.38
	8	1→2	177 260.99±0.40	177 261.07	1.69
	11	2→3	265 886.18±0.55	265 886.19	1.13
DCN	3	0→1	72 414.61±0.15	72 414.61	4.14
	6	1→2	144 827.86±0.30	144 827.84	2.07
	9	2→3	217 238.40±0.45	217 238.32	1 38
	12	3→4	286 644.67±0.60	289 644.67	1.04

[a] Corrected for electric quadrupole effects.
[b] Calculated with the B_0 and D_J given in Table VIII, and with $(eQq)_N = -4.73$ Mc/sec.

The method of construction of the 3-mm bolometer was suggested by K-band bolometer mounts available commercially from Polytechnic Research and Development Company. Wollaston wire, 0.00005 inch in diameter, was mounted on a mica wafer across a hole of about 0.035 inch diameter (the small dimension of the G-band wave guide employed), and the ends of the wire were secured in place on opposite sides of the wafer with Du Pont silver conductive coating No. 4810. After the etching of the Wollaston wire, the mica wafer was fitted between two short lengths of G-band wave guide, held in a suitable Lucite mount, in such a way that each piece of wave guide provided one electrical contact to the bolometer, as in the Polytechnic Research K-band unit. A thin mica window over one end of the assembled detector provided a vacuum seal at the end connected to the absorption cell; at the opposite end, a movable shorting plunger mounted with a linear O-ring seal was used for impedance matching and vacuum seal. During use, the sealed unit was evacuated to a pressure of 10^{-2} to 10^{-4} mm of mercury.

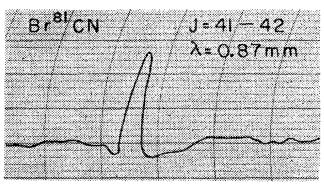

FIG. 3. Recorder tracing of the $J=41\rightarrow42$ transition of $Br^{81}CN$ at 0.87-mm wavelength obtained with a crystal detector and 14th harmonic of a 2K33 klystron.

TABLE II. N_2O.

Tube harmonic	Transition $J\rightarrow J+1$	Measured frequency (Mc/sec)	Calculated frequency[a] (Mc/sec)	Wavelength (mm)
4	3→4	100 491.74±0.20	100 491.74	2.99
5	4→5	125 613.73±0.25	125 613.71	2.39
6	5→6	150 735.13±0.30	150 735.04	1.91
7	6→7	175 855.72±0.35	175 855.59	1.71
8	7→8	200 975.26±0.40	200 975.25	1.49
9	8→9	226 093.81±0.45	226 093.88	1.33
10	9→10	251 211.33±0.50	251 211.34	1.19
11	10→11	276 327.50±0.55	276 327.53	1.09
12	11→12	301 442.38±0.60	301 442.30	0.99

[a] Frequencies calculated with the B_0 and D_J given in Table VIII.

Figure 2 shows a cathode ray trace of ClCN rotational line in the 1-mm region obtained with the silicon crystal detector followed by an ordinary P amplifier. Figure 3 shows a recording of a submillimeter ClCN line obtained with the same multiplier and detector and a phase lock-in detector and amplifier. Repeller modulation at 2000 cps was employed. These figures indicate the type of performance which can be expected from a well tuned system employing K-band klystrons for exciting

TABLE III. $Cl^{35}CN$.

Tube harmonic	Transition $J\rightarrow J+1$	Measured frequency ν_0(Mc/sec)[a]	Calculated frequency ν_0(Mc/sec)[b]	Wavelength (mm)
4	7→8	95 529.86±0.20	95 529.89	3.14
5	9→10	119 409.82±0.25	119 409.97	2.51
6	11→12	143 288.45±0.30	143 288.45	2.09
7	13→14	167 165.15±0.35	167 165.02	1.79
8	15→16	191 039.44±0.40	191 039.34	1.57
9	17→18	214 911.20±0.45	214 911.13	1.40
10	19→20	238 780.22±0.50	238 780.02	1.26
11	21→22	262 645.82±0.55	262 645.73	1.14
12	23→24	286 507.95±0.60	286 507.93	1.05
13	25→26	310 365.90±0.65	310 366.29	0.97
14[c]	27→28	334 219.5 ±1.5	334 220.5	0.89

[a] Corrected for electric quadrupole effects.
[b] Calculated with the B_0 and D_J given in Table VIII.
[c] Measured on recorder.

the multiplier. Actually, lines at 0.9 mm have been seen on the cathode-ray oscilloscope and measured with the video-type spectrometer, but this wavelength appears to be near the limit for video detection with K-band harmonics just as 0.77 mm appears to be near the limit of detection with K-band harmonics and the automatic recording method. Although several molecules have now been measured in the submillimeter region, measurements below 1 mm are still difficult and can be achieved only with optimum tuning conditions and the better $2K33$ klystrons. Measurements near or above 1 mm are entirely practical now, and indeed numerous studies have already been made[4,5] in the 1- to 2-mm region. Although the amount of power obtainable at 1.0 mm is certainly only a fraction of a microwatt, the intense absorption of molecules in the shorter millimeter region makes high power there unnecessary for practical spectroscopy.

TABLE IV. $Cl^{37}CN$.

Tube harmonic	Transition $J\rightarrow J+1$	Measured frequency ν_0(Mc/sec)[a]	Calculated frequency ν_0(Mc/sec)[b]	Wavelength (mm)
4	7→8	93 552.59±0.20	93 552.60	3.21
5	9→10	116 938.45±0.25	116 938.43	2.56
6	11→12	140,322.75±0.30	140 322.72	2.14
7	13→14	163 705.31±0.35	163 705.15	1.83
8	15→16	187 085.58±0.40	187 085.43	1.60
9	17→18	210 463.24±0.45	210 463.24	1.42
10	19→20	233 838.30±0.50	233 838.26	1.28
11	21→22	257 210.28±0.55	257 210.20	1.17
12	23→24	280 578.92±0.60	280 578.75	1.07
13	25→26	303 943.87±0.65	303 943.59	0.99

[a] Corrected for electric quadrupole effects.
[b] Calculated with the B_0 and D_J given in Table VIII.

TABLE V. $Br^{79}CN$.

Tube harmonic	Transition $J\rightarrow J+1$	Measured frequency ν_0(Mc/sec)[a]	Calculated frequency ν_0(Mc/sec)[b]	Wavelength (mm)
4	11→12	98 879.19±0.20	98 879.19	3.03
5	14→15	123 594.73±0.25	123 594.69	2.43
6	17→18	148 307.36±0.30	148 307.33	2.02
7	20→21	173 016.45±0.35	173 016.52	1.73
8	23→24	197 721.69±0.40	197 721.71	1.52
9	26→27	222 422.34±0.45	222 422.30	1.35
10	29→30	247 117.75±0.50	247 117.74	1.21
11	32→33	271 807.59±0.55	271 807.46	1.10
12	35→36	296 490.86±0.60	296 490.86	1.01
13[c]	38→39	321 167.1 ±0.65	321 167.39	0.93
14[c]	41→42	345 837.0 ±1.0	345 836.47	0.87

[a] Corrected for electric quadrupole effects.
[b] Calculated with the B_0 and D_J given in Table VIII.
[c] Measured on recorder.

MOLECULAR ROTATIONAL CONSTANTS

Tables I to VII give the frequencies of the various molecules which have been measured. For five of the species the measurements extended into the submillimeter range. Table VIII gives the molecular rotational constants derived from these with the formula,

$$\nu_0=2B_0(J+1)-4D_J(J+1)^3. \quad (1)$$

TABLE VI. $Br^{81}CN$.

Tube harmonic	Transition $J\rightarrow J+1$	Measured frequency ν_0(Mc/sec)[a]	Calculated frequency ν_0(Mc/sec)[b]	Wavelength (mm)
4	11→12	98 317.37±0.20	98 317.37	3.05
5	14→15	122 892.50±0.25	122 892.47	2.44
6	17→18	147 464.71±0.30	147 464.76	2.03
7	20→21	172 033.53±0.35	172 033.65	1.74
8	23→24	196 598.50±0.40	196 598.58	1.53
9	26→27	221 158.86±0.45	221 159.01	1.36
10	29→30	245 714.32±0.50	245 714.35	1.22
11	32→33	270 263.95±0.55	270 264.04	1.11
12	35→36	294 807.52±0.60	294 807.52	1.02
13[c]	38→39	319 345.52±1.0	319 344.2	0.94
14[c]	41→42	343 873.0 ±1.5	343 873.6	0.87

[a] Corrected for electric quadrupole effects.
[b] Calculated with B_0 and D_J given in Table VIII.
[c] Measured on recorder.

TABLE VII. OCSe.

Molecule	Tube harmonic	Transition $J\rightarrow J+1$	Measured frequency (Mc/sec)	Calculated frequency[a] (Mc/sec)	Wavelength (mm)
$OCSe^{76}$	4	11→12	97 637.78±0.20	97 637.78	3.07
	5	14→15	122 043.90±0.25	122 043.90	2.46
	6	17→18	146 447.90±0.30	146 447.80	2.05
	7	20→21	170 849.06±0.35	170 849.04	1.76
	8	23→24	195 247.17±0.40	195 247.17	1.54
	9	26→27	219 641.79±0.45	219 641.75	1.37
	10	29→30	244 032.33±0.50	244 032.34	1.23
$OCSe^{77}$	4	11→12	97 321.07±0.20	97 321.06	3.08
	5	14→15	121 647.98±0.25	121 648.00	2.46
	6	17→18	145 972.74±0.30	145 972.73	2.05
	7	20→21	170 294.80±0.35	170 294.81	1.76
	8	23→24	194 613.75±0.40	194 613.78	1.54
	9	26→27	218 929.21±0.45	218 929.21	1.37
$OCSe^{78}$	4	11→12	97 013.24±0.20	97 013.23	3.09
	5	14→15	121 263.28±0.25	121 263.25	2.47
	6	17→18	145 511.08±0.30	145 511.07	2.06
	7	20→21	169 756.27±0.35	169 756.26	1.77
	8	23→24	193 998.34±0.40	193 998.38	1.55
	9	26→27	218 236.97±0.45	218 236.99	1.37
	10	29→30	242 471.47±0.50	242 471.65	1.24
	11	32→33	266 701.93±0.55	266 701.93	1.12
$OCSe^{80}$	4	11→12	96 418.95±0.20	96 418.95	3.11
	5	14→15	120 520.40±0.25	120 520.43	2.49
	6	17→18	144 619.81±0.30	144 619.75	2.07
	7	20→21	168 716.41±0.35	168.716.46	1.78
	8	23→24	192 810.17±0.40	192 810.13	1.56
	9	26→27	216 900.38±0.45	216 900.34	1.38
	10	29→30	240 986.62±0.50	240 986.63	1.24
	11	32→33	265 068.60±0.55	265 068.60	1.13
	12	35→36	289 145.50±0.60	289 145.78	1.04
	13	38→39	313 217.57±0.65	313 217.76	0.96
$OCSe^{82}$	4	11→12	95 852.94±0.20	95 852.95	3.12
	5	14→15	119 812.89±0.25	119 812.96	2.50
	6	17→18	143 770.82±0.30	143 770.81	2.09
	7	20→21	167 726.08±0.35	167 726.09	1.79
	8	23→24	191 678.34±0.40	191 678.36	1.56
	9	26→27	215 627.18±0.45	215 627.18	1.39
	10	29→30	239 572.08±0.50	239 572.13	1.25
	11	32→33	263 512.90+0.55	263 512.78	1.14

[a] Calculated with the B_0 and D_J given in Table VIII.

[5] C. A Burrus and W. Gordy, Phys. Rev. **92**, 1437 (1953); **93**, 419 (1954); Burrus, Jache, and Gordy, Phys. Rev. **95**, 706 (1954); Blevins, Jache, and Gordy, Phys. Rev. **97**, 684 (1955); Burrus, Gordy, Benjamin, and Livingston, Phys. Rev. **97**, 1661 (1955).

TABLE VIII. Spectral constants.

Molecule	B_0 (Mc/sec)	D_J (Mc/sec)	q
HCN	$44\,315.99_1$	$9.04_0\times10^{-2}$	
DCN	$36\,207.42_0$	$5.73_8\times10^{-2}$	
N_2O	$12\,561.63_9$	$5.35_9\times10^{-3}$	23.73_6
$Cl^{35}CN$	5970.83_1	$1.66_3\times10^{-3}$	7.45_9
$Cl^{37}CN$	5847.24_3	$1.60_8\times10^{-3}$	7.16_6
$Br^{79}CN$	4120.22_1	$8.84_4\times10^{-4}$	3.91_5
$Br^{81}CN$	4096.80_8	$8.71_6\times10^{-4}$	3.86_9
$OCSe^{76}$	4068.43_8	$6.84_6\times10^{-4}$	
$OCSe^{77}$	4055.24_1	$6.83_4\times10^{-4}$	
$OCSe^{78}$	4042.41_3	$6.77_1\times10^{-4}$	
$OCSe^{80}$	4017.64_9	$6.69_5\times10^{-4}$	3.17_2
$OCSe^{82}$	3994.06_4	$6.64_0\times10^{-3}$	

For some, corrections for nuclear quadrupole effects were necessary as indicated in the tables. Approximate values of the stretching constants, D_J, have been obtained for most of these molecules from earlier measurements on lower J transitions. Only the 0→1 transitions of HCN and DCN have been previously measured. Because of the increase of the centrifugal stretching with rate of rotation, the centrifugal stretching term, $4D_J(J+1)^3$, becomes large and D_J can be accurately measured in the 1-mm region. In the present work, transitions up to $J=41\rightarrow42$ were measured for $Br^{79}CN$ and $Br^{81}CN$. Here the deviations caused by the centrifugal stretching term of Eq. (1) amount to 250 Mc/sec. No deviation from Eq. (1) was detected in the present work. Extension to still higher J, or more accurate measurement, is required to detect higher order centrifugal stretching effects.

Table IX lists the frequencies which are measured for l-type doublets of molecules in the first excited degenerate bending vibrational mode. According to Nielsen's theory,[6] the splitting of rotational levels by the interaction between vibration and rotation are given by

$$\Delta E=hqJ(J+1). \tag{2}$$

For $J\rightarrow J+1$ transitions the doublet separation is

$$\Delta\nu=2q(J+1), \tag{3}$$

where q is the l-type doubling constant measured in frequency units. If higher order effects not included in Eq. (2) are neglected, $\Delta\nu/[2(J+1)]$ should have the same value for different rotational states. It was found to be constant within the limits of experimental error for the transitions measured (up to $J=29\rightarrow30$) for $Br^{79}CN$. A slight deviation in q with increasing J has been found[7] for HCN, where the l-type doubling is so large that direct transitions between the l-doublets (with no change in J) are observable in the centimeter wave region.

TABLE IX. l-type doublets.

Molecule	Tube harmonic	Transition $J\rightarrow J+1$	Measured frequencies[a] (Mc/sec) lower	upper	$q=\frac{\Delta\nu}{2(J+1)}$
$Cl^{35}CN$	4	7→8	95 731.52	95 850.88	7.46_0
	5	9→10	119 662.15	119 811.35	7.46_0
	6	11→12	143 591.01	143 770.23	7.46_8
	7	13→14	167 517.88	167 726.78	7.46_1
	8	15→16	191 442.66	191 681.13	7.45_2
	9	17→18	215 364.77	215 633.04	7.45_2
	10	19→20	239 283.85	239 582.25	7.46_0
$Cl^{37}CN$	4	7→8	93 751.28	93 865.98	7.16_9
	5	9→10	117 186.54	117 329.90	7.16_8
	6	11→12	140 620.55	140 792.59	7.16_8
	7	13→14	164 052.55	164 253.26	7.16_8
	8	15→16	187 482.50	187 711.52	7.15_7
	9	17→18	215 769.51	216 027.44	7.16_5
$Br^{79}CN$	4[b]	11→12	99 108.45	...	...
			99 109.06	99 203.06	3.91_7
			99 110.12	99 204.09	3.91_5
			99 110.75	99 204.70	3.91_5
	5[b]	14→15	123 881.78	123 999.22	3.91_5
			123 882.90	124 000.30	3.91_3
	6[b]	17→18	148 652.01	148 792.99	3.91_6
			148 652.83	148 793.79	3.91_6
	7	20→21	173 418.77	173 583.26	3.91_6
	8	23→24	198 181.25	198 368.79	3.91_4
	9	26→27	222 939.11	222 150.44	3.91_4
	10	29→30	247 691.48	247 925.95	3.90_8
$Br^{81}CN$	4[b]	11→12	98 545.65	98 638.49	3.86_8
			98 546.18	98 639.01	3.86_8
			98 547.08	98 639.95	3.87_0
			98 547.63	98 640.42	3.86_6
	5[b]	14→15	123 178.33	123 294.38	3.86_8
			123 179.40	123 295.31	3.86_4
	6[b]	17→18	147 807.77	147 947.11	3.87_1
			147 808.49	147 947.85	3.87_1
	7	20→21	172 434.07	172 596.70	3.87_2
	8	23→24	197 055.84	197 241.70	3.87_2
	9	26→27	221 673.17	221 881.84	3.86_4
$OCSe^{80}$	4	11→12	96 546.60	96 622.76	3.17_3
	5	14→15	120 679.98	120 775.11	3.17_1
	6	17→18	144 811.06	144 925.26	3.17_2
	7	20→21	168 939.60	169 072.81	3.17_2
	8	23→24	193 065.08	193 217.26	3.17_0
	9	26→27	217 186.90	217 358.18	3.17_2
N_2O	4	3→4	100 531.65	100 721.58	23.74_1
	5	4→5	125 663.69	125 900.99	23.73_0
	6	5→6	150 794.98	151 079.83	23.73_8

[a] Measured frequencies not corrected for electric quadrupole effects in ClCN and BrCN.
[b] Listed components due to electric quadrupole effects sufficiently resolved at these frequencies to be measured.

[6] H. H. Nielsen, Revs. Modern Phys. **23**, 90 (1951).

[7] J. F. Westerkamp, Phys. Rev. **93**, 716 (1954).

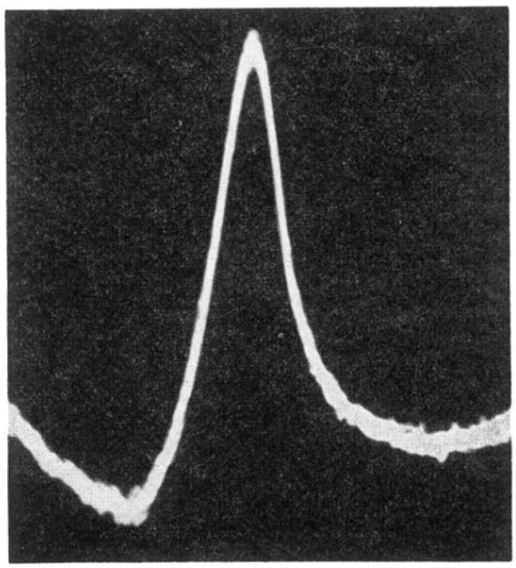

FIG. 1. Cathode-ray tracing of the $J=7\rightarrow 8$ transition of OCS at 3.08-mm wavelength as obtained with a bolometer detector.

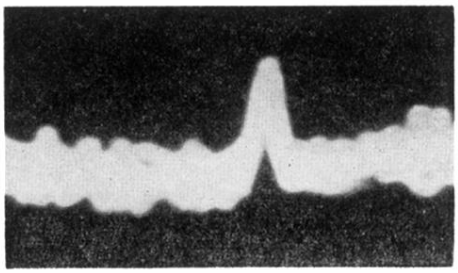

FIG. 2. Cathode-ray tracing of the $J=23\rightarrow24$ transition of $Cl^{35}CN$ at 1.05-mm wavelength obtained with a crystal detector and the 12th harmonic power of a $2K33$ klystron.

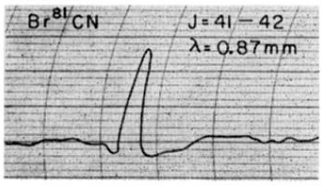

FIG. 3. Recorder tracing of the $J=41\rightarrow42$ transition of $Br^{81}CN$ at 0.87-mm wavelength obtained with a crystal detector and 14th harmonic of a 2*K*33 klystron.